Spectrochimica Acta Part B: Atomic Spectroscopy 181 (2021) 106213

Contents lists available at ScienceDirect

Spectrochimica Acta Part B: Atomic Spectroscopy

journal homepage: www.elsevier.com/locate/sab

Laser-induced breakdown spectroscopy as enabling key methodology for inverse production of end-of-life electronics

Reinhard Noll [a,b,*], Cord Fricke-Begemann [a], Frederik Schreckenberg [a]

[a] Fraunhofer-Institut für Lasertechnik (ILT), Steinbachstraße 15, 52074 Aachen, Germany
[b] RWTH Aachen University, Lehrstuhl für Lasertechnik (LLT), Steinbachstraße 15, 52074 Aachen, Germany

ARTICLE INFO

Keywords:
LIBS
Scanning LIBS
Fusion of geometric and spectroscopic data
Inverse production
Valuable materials
Sorting

ABSTRACT

Inverse production strives for a selective dismantling of industrial mass products at their end-of-life (EOL) with the goal to generate highly enriched fractions of valuable materials for subsequent tailored recovery procedures. Since in many cases there is only fragmentary or even no information available about the chemical composition of such EOL-products and their components, there is a need for a fast, inline, multi-element, stand-off analyzing methodology, that can be integrated in an inverse production line. Within the European project ADIR, LIBS was studied to identify valuable materials in electronic components and to allocate this analytical information to the location of the measuring object on the printed circuit boards of the EOL-product. The fused data set of physical – gained via 2D, 3D geometry measurements – and chemical data allows for a selective disassembly and sorting of such electronic components. This paper describes the developed scanning LIBS method, gained results, and the integration of the LIBS measurements in the worldwide first inverse production line to process printed circuit boards of servers and cell phones.

1. Introduction

Inverse production strives for a selective dismantling of industrial mass products at their end-of-life (EOL) with the goal to generate highly enriched fractions of valuable materials for subsequent tailored recovery procedures. This is an essential step to establish efficient circular economy concepts. Whereas for conventional industrial production input materials and components are – as a rule – known, the situation of a process line selectively treating EOL electronics is much more challenging.

The variety of features of the material to be processed is very broad and often there is limited or no information available about the chemical composition. Hence there is a need for a fast analyzing methodology to set-up the data space for inverse production as a key element of an inverse production line to automatically dismantle and sort valuable components from EOL electronics.

Within the European project ADIR, a consortium of R&D institutes and companies has developed processes and machines to demonstrate the feasibility of a novel approach for an automated selective disassembly of consumer and professional EOL electronics [1]. The target of the ADIR project was to use selective physical separation methods to gain highly enriched sorting fractions of valuable materials for a tailored recycling and recovery of these substances.

In that context, LIBS was studied to identify inline – i.e. within a process line of inverse production - valuable materials in electronic components and to allocate this analytical information to the location of the measuring object within the structure of the EOL electronics, i.e., the printed circuit boards (PCBs). Geometry data gained by optical 2D- and 3D-measurements are fused with LIBS data and deployed for a subsequent selective disassembly and sorting of electronic components with high contents of valuable materials such as tantalum. The developed scanning LIBS method, gained results and the integration of the LIBS measurements in the worldwide first inverse production line to process EOL printed circuit boards and cell phones are described in the following.

Several studies on LIBS referring to the topics waste electronic and electric equipment (WEEE), PCB and recycling were published in the last two decades. Two queries in the Web of Science were carried out (Feb. 2021) using as search terms: i) “laser-induced breakdown spectroscopy” AND “WEEE” AND “laser” AND “recycling”; ii) “laser-induced breakdown spectroscopy” AND “printed circuit boards”. Query i) yielded 8 hits (see references [2–9]), query ii) yielded 10 hits, from which two are

* Corresponding author at: Fraunhofer-Institut für Lasertechnik (ILT), Steinbachstraße 15, 52074 Aachen, Germany.
E-mail address: reinhard.noll@ilt.fraunhofer.de (R. Noll).

https://doi.org/10.1016/j.sab.2021.106213
Received 24 February 2021; Received in revised form 7 May 2021; Accepted 8 May 2021
Available online 11 May 2021

only marginally related to the search terms (remaining hits see: [10–14] and [7–9]).

Polymer samples containing heavy metals and brominated flame retardants – as they are used for housings of WEEE – were studied by LIBS using single and double pulses [2]. Detection limits (3*s*-criterion) ≤ 50 μg/g were achieved for the analytes Cd, Cr, Hg, Pb, Sb, and for Br ≤ 15 mg/g. The developed method was evaluated in a pilot sorting plant with waste monitors moving on a belt conveyor. LIBS combined with chemometrics was studied to classify polymer and PCB parts which were cut from mobile phones [3]. Spectra of PCBs (the board itself, not the electronic components mounted on the board) showed signals attributed to Cu, Ba, Si, and Mg. In [4] the same group studied polymeric fractions of scrap from mobile phones using LIBS and chemometric methods with the goal to classify the origin and manufacturer of polymeric scraps of these devices. Classification models based on a K-nearest neighbor approach (KNN) showed the highest degrees of correct classifications of ≥92% for black and white polymers.

E-waste polymers arcylonitrile-butadiene-styrene (ABS), polystyrene, polyethylene, polycarbonate (PC), polypropylene (PP), and polyamide (PA) were studied using emission lines of C, H, N, O, and the molecular C2-band with LIBS and chemometric tools to identify the polymer matrix [5]. With a K-nearest neighbor approach average accuracies of 98% were achieved. The capability of LIBS combined with partial least square (PLS) regression to determine the PC and ABS content in their blends originating from plastic scraps of e-waste was shown in [6]. Reference [7] provides a review of the contribution of LIBS to the chemical inspection of polymers and PCBs from WEEE. The studies treating PCBs are focused on solder masks, their stripping by laser irradiation to expose the copper underneath and hyperspectral imaging for the identification of the location of 18 elements in PCBs (for the latter aspect see [8]).

A parallel factor analysis was studied to characterize base (Al and Cu) and noble (Au and Ag) elements on a PCB. Up to ten laser pulses with 100 mJ pulse energy were applied at each measuring spot at cut-out fragments of a PCB each having the dimensions 10 × 10 mm^2 [8]. A raster measurement of 4 × 4 spots is performed at these fragments with a distance between neighboring measuring points of 1 mm. Relative concentration maps calculated for Cu and Al are shown. An allocation of the evaluated raster data to electronic components on the PCB is not given.

Five calibration methods were evaluated comparatively to analyze the content of Al and Pb in ground and pressed samples of PCBs from desktop computers [9]. In the studied concentration ranges (Al: 3–55 g kg^{-1}; Pb: 0.7–12 g kg^{-1}) matrix-matching calibration and calibration-free method generally allowed accurate values to be obtained for both analytes.

A compositional mapping by LIBS using the second harmonic of a Nd:YAG laser and two translational stages to which the sample is fixed, showed that the flat copper conductor pattern from a PCB can be resolved [10]. For a measuring field of 5 × 5 mm^2 a raster scan was performed with 100 × 100 pixels taking up to 120 min measuring time.

Reference [11] presented a raster scan using a 12 mm long and 42 μm wide laser line to generate mappings of Ni and Cu from the edge connectors of PCBs. The spatial distribution of relative intensities of Ni- and Cu-lines was measured in a field of 4 × 1.4 mm^2; depth profiles are gained up to a depth of ca. 1500 μm corresponding to a sequence of 30 laser pulses.

Contacts of desktop/notebook memory chips and pins of desktop processors were studied to detect Au and Ag by a sequence of 10 to 30 pulses on a measuring spot [12]. Principle component analysis (PCA) and comparative measurements with scanning electron microscopy energy-dispersive X-ray analysis (SEM-EDX) were conducted.

The metal composition of a PCB from a mobile phone was studied with a raster scan in a field of 30 × 40 mm^2, step size 1 mm, and up to 10 laser pulses were irradiated per spot [13]. Various PCA steps were performed for 18 elements to evaluate their lateral distribution and their depth profile (up to ca. 20 μm). Obtained score maps and loading values were used in combination with a semi-quantitative SEM-EDX to estimate element concentrations. Hyperspectral images were calculated as false color maps of loading values indicating areas of negative (Si) and positive scores (Ni).

Table 1
Top 13 list of end-of-life cell phones (class i)).

No.	Manufacturer	Model
1	Nokia	6230i
2	Nokia	3410
3	Nokia	3210
4	Nokia	3510
5	Siemens	C25
6	Nokia	5110
7	Nokia	3330
8	Nokia	6230
9	Nokia	1208
10	Siemens	A55
11	Samsung	GT-SS230
12	HTC	One mini 2
13	Samsung	Galaxy S4

Table 2
Top 10 list of end-of-life PCBs from servers (class ii)).

No.	Manufacturer	Model
1	Hewlett Packard	DL 380 G5
2	Siemens	RX 300 S2
3	Hewlett Packard	Proliant DL 380 G5
4	Hewlett Packard	DL 360 G6
5	Hewlett Packard	DL 380 G6
6	Siemens	RX 600 S5
7	Hewlett Packard	DL 360 G5
8	Hewlett Packard	DL 580 G5
9	Hewlett Packard	DL 580 G6
10	Siemens	RX 300 S3

In [14] the elemental content of solder mask samples used for homemade PCBs was studied with spectroanalytical techniques: inductively coupled plasma-optical emission spectrometry (ICP-OES), inductively coupled plasma-mass spectrometry (ICP-MS) and LIBS. For LIBS samples were prepared on a Teflon foil (PTFE) held between an Al-holder and a glass support. Semi-quantitative LIBS analyses were performed for Ba, using as reference ICP-OES data.

In the cited papers [4–6,8,10–14] scanning was performed by moving the sample on *xy*-stages relative to the stationary laser beam (e.g. 30 × 40 mm^2 in [13]). In contrast, in this paper we present a scanning LIBS method where the laser beam is deflected by galvo-scanners thus enabling fast scans of PCBs with dimensions of up to 500 × 500 mm^2 and height variations of up to 60 mm. Electronic components mounted on the PCB are analyzed selectively to identify their internal composition. Combined with 2D/3D geometry data of these components a fused data set is generated, enabling an assessment of the volume and content of valuable material inside this electronic component. To obtain highly enriched material fractions, this data is deployed for a subsequent selective extraction of that component using laser desoldering.

2. Measuring objects

Two classes of input material were studied: i) printed circuit boards from cell phones, ii) PCBs from servers and computers. Since the variety of different PCB types is very large, a representative selection was defined covering abundant types of PCBs from older types of cell phones (so-called brick phones) as well as from smart phones. Moreover, the availability of the various items in a current recycling stream was considered. Based on a collection of 15,000 cell phones and 1600 large PCBs from servers, for class i) a top 13 list was defined and for ii) a top 10 list [15], see Tables 1, 2.

The printed circuit boards of class i) and ii) span a wide range of geometries with lateral dimensions from 47 × 108 mm^2 (cell phone PCB) to 500 × 370 mm^2 (server PCB).

The target components are mainly capacitors and surface acoustic wave filters owing to tantalum, integrated circuits for gold and unbalance masses of vibration alerts for tungsten. The considered size range of the capacitors in their packaging format as surface mounted devices (SMD) goes down to the dimensions 1 × 0.5 × 0.5 mm^3. In general, from the external appearance of e.g. capacitors (labeling, color of housing) it cannot be seen whether a tantalum capacitor is present. Moreover, data from the manufacturers of the PCBs or the electronic components with respect to the chemical composition are not available.

To illustrate the heterogeneous internal structure of such components, Fig. 1 shows a microscope image of the typical cross section of a SMD capacitor, in this case a tantalum capacitor. A SEM-EDX reveals different materials as epoxy resin molding for the housing (yellow), electrodes made of copper, silver contact layers and as dominant part of the volume the dielectric consisting of tantalum oxide (Ta_2O_5).

In order to identify the composition of the dielectric of such capacitors with LIBS, an adequate measuring location has to be found and the dielectric inside the component housing and partially underneath metallic electrodes and contact layers has to be accessed.

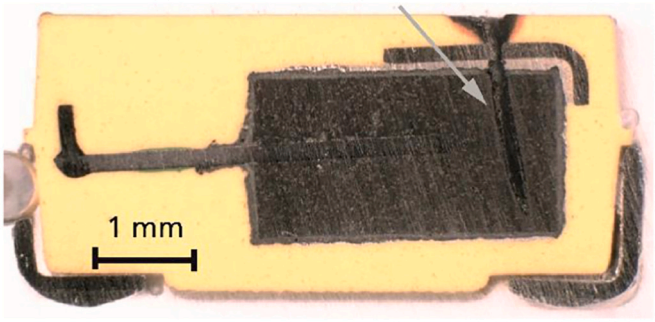

Fig. 1. Cross section of a SMD tantalum capacitor. On the right a blind boring (indicated by arrow) generated by laser ablation is seen penetrating a contacting electrode and ending within the dielectric of the capacitor (dark brown). (For interpretation of the references to color in this figure legend, the reader is referred to the web version of this article.)

3. Set-up of scanning LIBS combined with 2D-, 3D-geometry measurements

A scanning LIBS system combined with 2D-, 3D-geometry measurements was developed. Fig. 2 shows the set-up and illustrates a measuring sequence in a time series t_0, t_1 and t_2. The beam of a Nd:YAG laser (shown in red for t_2) is guided via a focus shifter to a galvanometer scanner optics (SO) directing the focused laser beam to any point within a measuring volume (MV) with the dimensions 500 × 500 × 60 mm^3. The laser source runs at a repetition rate of 100 Hz and can be operated in two modes: i) ablation pulses, so-called free-running laser generating pulse bursts within a time interval of ≈100 μs; ii) Q-switch mode generating pulses with a duration of 15 ns used for LIBS measurements. Also the Q-switch pulses cause an ablation, however for the pulses of mode i) – with an extended pulse duration – the ablation depth is much greater (hence we used the terminology 'ablation pulses' for this mode). For an aluminium sample 10 ablation pulses irradiated at one spot generate a crater with a depth of (1 ± 0.3) mm, whereas for 10 Q-switch pulses the depth is below 50 μm.

The PCB to be measured is placed and clamped at time t_0 on a translation stage (implemented as a drawer) in the *xy*-plane. Then the drawer moves in positive *y*-direction (t_1) and the geometry of the measuring object is measured in 2D with a strip-shaped white light illumination (WI) and a color line camera (CC). Simultaneously, the 3D shape is measured by projection of a laser line (LL) and observation of this line under an angle with a further camera (3D) using the triangulation principle (laser light section method or 2D laser triangulation). With this information the LIBS measurements are started (t_2), the LIBS laser beam can be directed by the scanner sequentially to any point of the measuring object inside the measuring volume and conduct local LIBS measurements at selected components, small line scans on single objects or raster scans of the whole PCB.

For large PCBs, the translation stage performs several forward and backward movements in *y*-direction, whereby the position of the 2D and 3D cameras is adjusted transversely (*x*-axis in Fig. 2) to the axis of movement between scans in order to obtain adjoining partial images. The up to three partial images are combined by software to form an overall image of the measuring object with high spatial resolution.

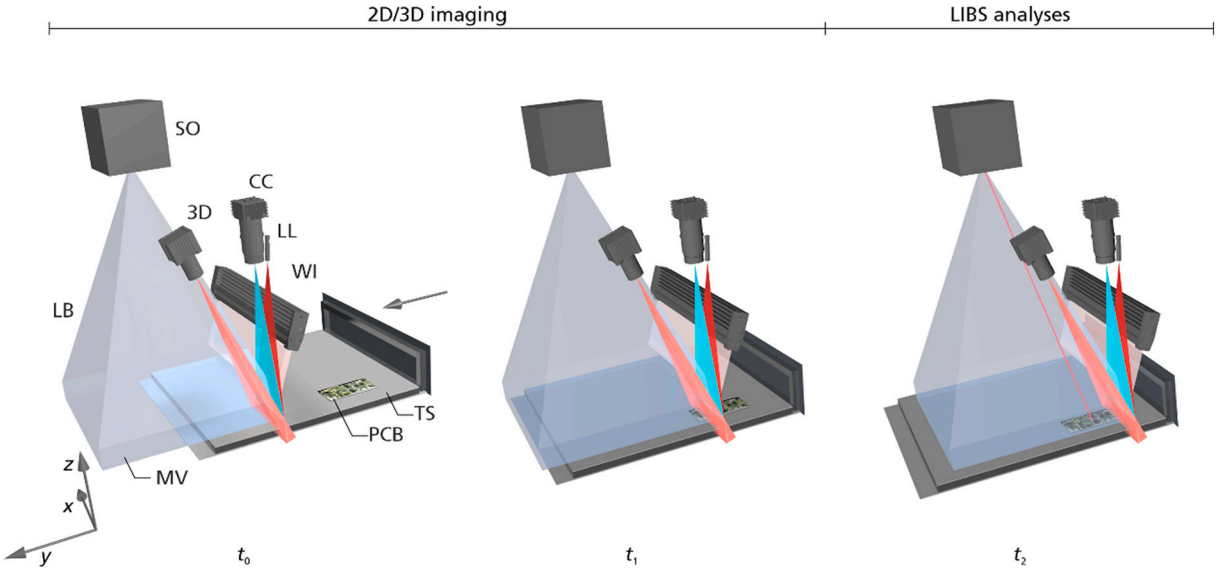

Fig. 2. Scanning LIBS set-up combined with 2D-, 3D-geometry measurements. SO scanner optics with orthogonal galvometer-driven mirrors, LB region of the scanned laser beam for LIBS, MV measuring volume for LIBS, CC color camera, LL laser line for 3D measurements, WI white light illumination, 3D camera for laser light section measurement, PCB printed circuit board as measuring object, TS translation stage moving in *y*-direction.

Table 3
Data of scanning LIBS set-up with 2D, 3D geometry measurements.

Item	Data
Translation stage	max. speed 1000 mm/s
2D camera	line array, 4096 pixels, 3 colors
3D camera	laser line section, 1280 × 1024 pixels
2D/3D measuring time	< 30 s for a 500 × 500 mm^2 PCB
Scanner for LIBS laser	two-axis mirror galvanometer, axial focus shifter, vertical distance to bottom of MV: 650 mm
MV, scan field including focusing	500 × 500 × 60 mm^3
LIBS laser	1064 nm, ~100 mJ, 100 Hz; ablation pulses ≈100 μs, Q-switch pulses 15 ns
Laser spot diameter	≈ 1 mm (nearly constant within measuring volume due to axial focus shifter and maximum deflection angles of <20°)
Spectrometer	Paschen-Runge system with 8 CCD line arrays along the Rowland circle, diameter of Rowland circle: 500 mm; spectral range 234–545 nm, spectral resolution δλ ≈ 15 pm@234 nm, multi-channel signal electronics

MV measuring volume.

The radiation emitted from the plasma propagates via the two galvanometer mirrors to a dichroic mirror (75 × 50 mm^2), passes this mirror and is then coupled by a lens ($f = 150$ mm) to a multimode fiber (⌀ = 600 μm, length 5 m). The fiber guides the measuring light to the entrance slit of a Paschen-Runge spectrometer equipped with eight CCD line arrays.

Table 3 summarizes the data of the set-up.

4. Results of 2D, 3D geometry and LIBS measurements of electronic components on printed-circuit boards

A prerequisite for LIBS measurements on the 3D surface profile of a PCB are highly resolved geometry measurements to locate the position, orientation and height of electronic components on the PCB. With the set-up of Fig. 2, 2D images of large server PCBs are gained resolving also very tiny objects with characteristic dimensions down to 1 mm within the overall image with extensions of 500 × 420 mm^2. The estimated spatial resolution in the *xy*-plane amounts to ≤60 μm.

The coordinates (*x, y*) of a component are not sufficient to assure that the LIBS laser beam is directed and focused to a defined location at the upper surface of an electronic component due to the required deflection angles of the scanned LIBS laser beam and the different heights of the respective electronic components. Fig. 3 shows a 3D color-encoded image of a PCB from a cell phone taken with the set-up of Fig. 2. The estimated height resolution is ≤500 μm.

The gained 2D and 3D data are fused to obtain a comprehensive digital representation of the PCB. Based on this data set the (*x, y, z*) coordinates of the electronic components as well as their respective volume are deduced. The coordinates are deployed to control the focus shifter and the scanner for the LIBS laser beam in order to perform spectroscopic measurements of selected components at defined positions.

In a first step, a series of raster scans of a complete PCB from a cell phone were performed at a fixed step size in *x*- and *y*-direction of 2 mm in order to get a qualitative overview where to find electronic components containing e.g. tantalum. For this measurement a different laser source with the following parameters was used: 1064 nm, 15 Hz with a tailored pulse train consisting of ablation pulses with in total 300 mJ followed by double pulses with 250 mJ (interpulse separation of 6 μs). Fig. 4 shows a series of such scans with false color presentations of the elemental signals of tantalum and copper (arbitrary units; the color scale corresponds to the sum of background corrected analyte line intensities gained from normalized spectra; for each analyte element a scale results whose maximum value corresponds to the highest summed intensity for all depths). The first raster scan – here denoted as 'depth = 1' – already

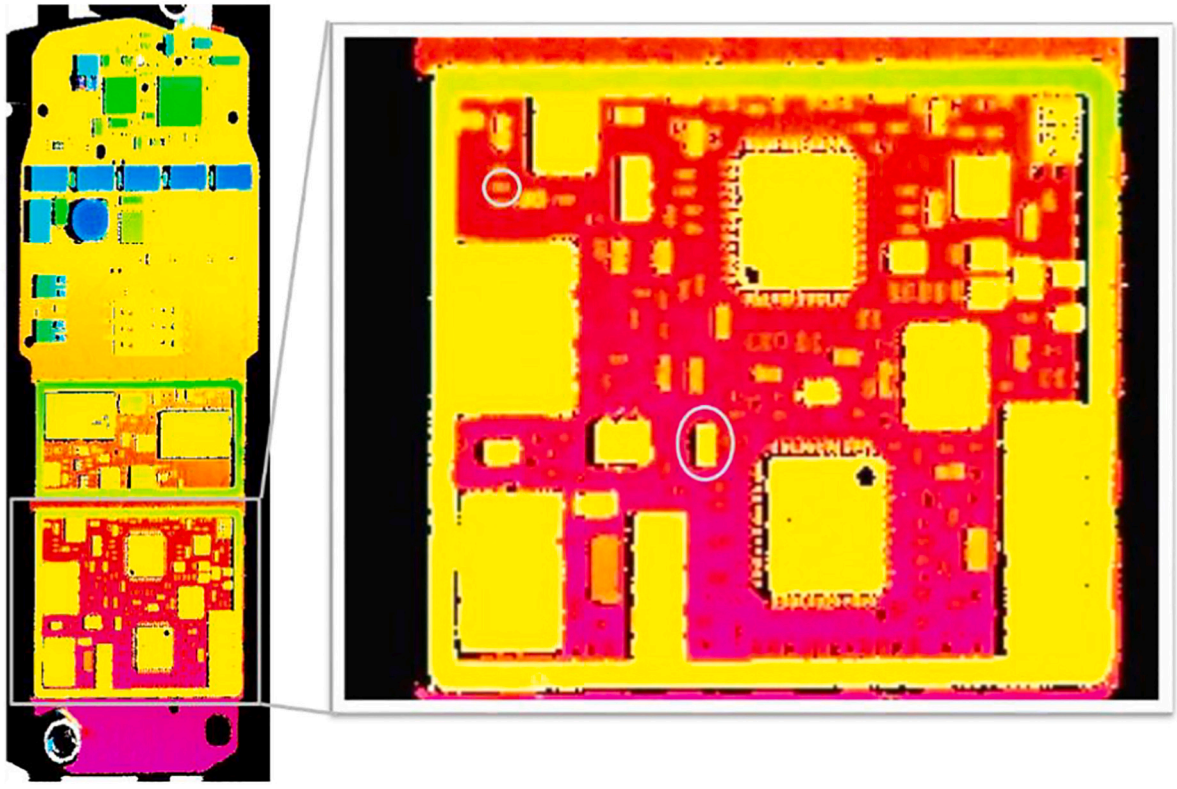

Fig. 3. 3D image of the PCB of a cell phone, heights are color-coded. Left: overall view of the PCB; right: enlarged section of the rectangle marked on the left image. Markings (circle, ellipse) show SMD components with the dimensions 1 × 0.5 × 0.5 mm^3, 2 × 1.5 × 1.2 mm^3, respectively.

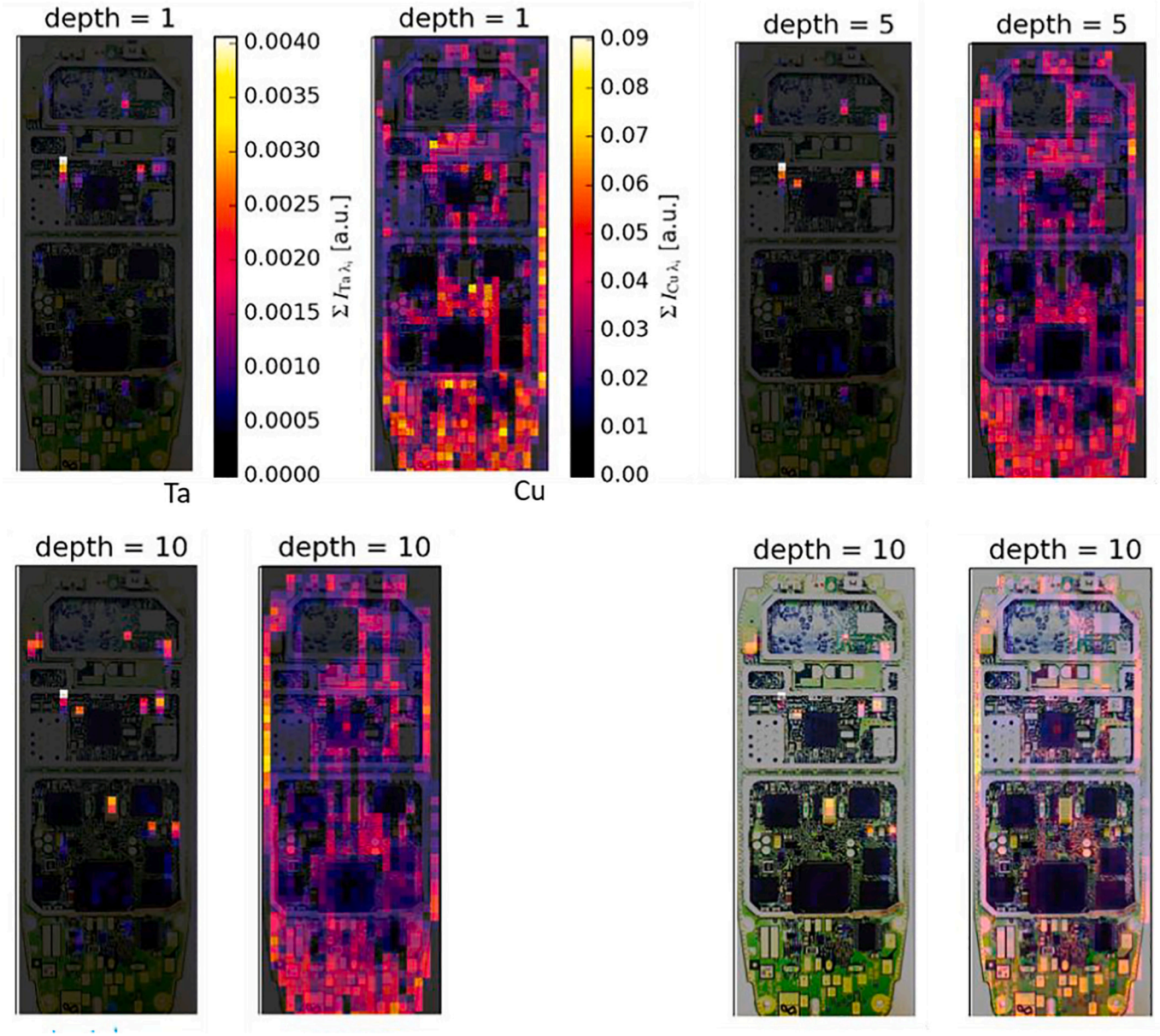

Fig. 4. LIBS raster scans with a step size of 2 mm of a complete PCB from a cell phone. Top, left: tantalum and copper mapping gained with a single laser pulse train at each measuring position (here called 'depth 1'). Top, right: tantalum and copper mapping for the fifth scan with the same raster. Bottom, left: tantalum and copper mapping for the 10th scan. Bottom, right: overlay presentation of the 10th raster scans with a color photo of the original PCB.

reveals some positions where significant tantalum emission signals occur. Copper signals are visible at much more locations, they are simply a consequence of the copper layers of the PCB. It is not possible to state the local ablation depth at the various measuring points of the scan since the ablation behavior depends on the respective local material composition and will be, e.g., larger for soft, organic materials and smaller for metals. Since tantalum and copper can already be seen for the 'depth = 1'-scan, we estimate that the ablation depths for a single pulse train (i.e. the sum of ablation pulses and double pulse) varies in the range of about 50 to 200 µm.

By repetition of the raster scans the laser ablation proceeds and reaches deeper regions. At the fifth and tenth raster scan (depth = 5 and 10) even more locations become visible with a clear tantalum signal. Finally, the chemical images are overlayed with the color photograph of the PCB taken prior to the LIBS measurements – see bottom, right of Fig. 4 – which allows to allocate the dimensions of the respective electronic components comprising the target valuable element.

Due to the inhomogeneity of the measuring objects, cf. e.g. Fig. 1, quantitative analytical measurements based on calibrations are rather complex (see stated references in Sect. 1). Hence, a semi-quantitative approach was deployed with the following steps:

a) LIBS measurements of a set of eight different homogeneous reference samples each having a high content (> 50 m.-%) of one of the target analytes (Cu, W, Ta, Nb, Nd, Au, Pd, Ag). These measurements yield average line intensities (background corrected) for the target element *j*: $\langle I^j_{\mathrm{hi}} \rangle$, where the index "hi" denotes measurements at a reference sample with high analyte content *j*. An example of such a spectrum is shown in Fig. 5. Table 4 lists the reference samples used.

b) LIBS measurements of a set of five different homogeneous reference samples, consisting of materials of low interest ("disturber"), and used here as "zero samples" (sample no. 9–13 in Table 4) with respect to the analytes listed in a): $\langle I^j_{\mathrm{lo}} \rangle$, where the index "lo" denotes the

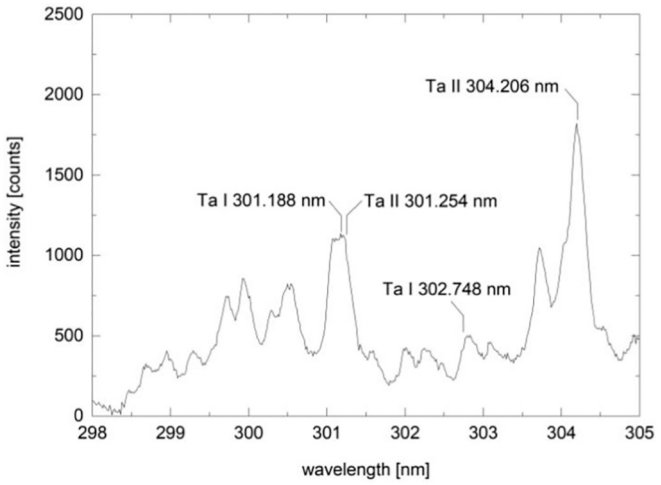

Fig. 5. Exemplary spectrum of the tantalum reference sample. Atomic and first ionic emission llines are indicated according to [18].

Table 4
Reference samples used.

No.	Target element, disturber	Composition
1	copper	99.99 m.-%
2	tungsten	mostly W, other elements <100 µg/g
3	tantalum	↑
4	niobium	↑
5	neodymium	magnet with Nd, Fe, B
6	gold	99.99 m.-%
7	palladium	99.99 m.-%
8	silver	↑
9	disturber Fe	./.
10	disturber Ti	./.
11	disturber Al/Mg	./.
12	disturber brass	./.
13	disturber limestone	./.

m.-% mass fraction, ↑ mostly target element >20–50 m.-%, ./. low or no content of target element.

Table 5
Analyte lines used for the LIBS score evaluation.

Analyte line	Wavelength [nm]
Ag I	328.068
Ag I	338.289
Au I	267.595
Cu I	324.754
Cu I	327.396
Nb I	407.973
Nd II	430.357
Pd I	348.977
Ta II	301.254
W I	400.875

Line data are taken from [18].

measurements at these five reference samples with very low (< 1 m.-%) or even no content of the target element j.

c) For a series of LIBS measurements at one location of an electronic component, a set of analyte intensities is gained: I_i^j, where j denotes the target analyte element and i is a counter with $i \in [1,K]$, K number of measurements at this location (for Fig. 4 we used: $K = 10$). The reference sample data is used to calculate a LIBS score value defined as: $ls_i^j = (I_i^j - \langle I_{lo}^j \rangle)/(\langle I_{hi}^j \rangle - \langle I_{lo}^j \rangle)$. Only those values ls_i^j are taken which lie in the interval $ls_i^j \epsilon$ [0,1].

The LIBS score ls_i^j is a semi-quantitative dimensionless measure of the content of a target analyte j in an inhomogeneous measuring object based on reference measurements of sets of homogeneous high-content and zero-content samples. Table 5 gives a list of the analyte lines detected and used for the corresponding LIBS score evaluation.

Besides global raster scans (see Fig. 4) local scans were performed for a single electronic component in order to gain information where the valuable material is located inside such a component. Different measuring sequences were studied for the global and local scans, Table 6 shows an overview.

Table 6
Measuring sequences studied.

Sequence	Pulse burst	Pulse energy per measuring spot	Purpose	Example
i)	AP + DP per spot	300 mJ + 250 mJ	element mappings of whole PCBs, global raster scan, step size 2 mm	Fig. 4
ii)	AP for all raster spots, SP for all raster spots	100 mJ, 100 mJ	measurements at single electronic components in a 20 × 4 local raster scan, step sizes 270 µm, 100 µm	Fig. 6
iii)	AP for all raster spots, SP at central raster spot	100 mJ, 100 mJ	measurements at single electronic components at a predefined position, local raster scan (e.g. 3 × 3), step size 200 µm	Fig. 7

AP ablation pulses; for LIBS measurements: DP double pulse, SP single pulse.

Fig. 6 illustrates the individual phases of a local scan measurement. The left picture shows a SMD component (package size EIA 7343–20, 7.3 × 4.3 × 2.0 mm^3) – a tantalum capacitor – as a selected electronic component. The picture in the middle shows this component after penetrating the housing by a linear raster scan of laser ablation pulses. Finally, within the trench created, laser measuring pulses are irradiated to analyze the exposed inner material.

The figure on the right shows the determined LIBS scores for the element tantalum for a measuring grid with 20 × 4 measuring points (step size $\Delta y = 270$ µm, $\Delta x = 100$ µm; measuring time per measuring point: 0.5 s, number of spectra per spot: 50). In the lower part of the graph, i.e. for coordinates 3.6 mm < y < 6.3 mm, the LIBS scores reach values of up to 0.6. The observed asymmetric distribution of the tantalum pentoxide dielectric within the SMD capacitor is consistent with the results of measurements on longitudinal sections of such capacitors, which were carried out with SEM-EDX (cf. Fig. 1). These show that the dielectric only partially fills the volume of the component and that its center of gravity is shifted towards the cathode (which is located at the bottom edge of the component in Fig. 6, left). The volume fraction filled by the cell body varies strongly depending on the electronic properties of the component.

Fig. 7 shows exemplarily LIBS score results gained for a tantalum capacitor at a predefined position. When only LIBS measurement pulses are applied to the surface of the component (top row), the plastics housing is just penetrated and the elements Cu and Ni are detected originating from the upper electrode, see bar diagram top, right.

When an additional laser pre-ablation process step is included in the measurement sequence (bottom row; see Table 6 for laser pulse parameters), the electrode is penetrated and the sintered capacitor cell body is reached. The LIBS score clearly indicates the presence of tantalum, distinguishing the component from a similar looking niobium capacitor.

Together with the measured volume of the electronic component (based on the 2D and 3D images), the LIBS scores provide an assessment basis to classify the composition of the component and to decide whether a dismantling of that component is meaningful. The considered decision criteria are: a) identification of valuable material in an

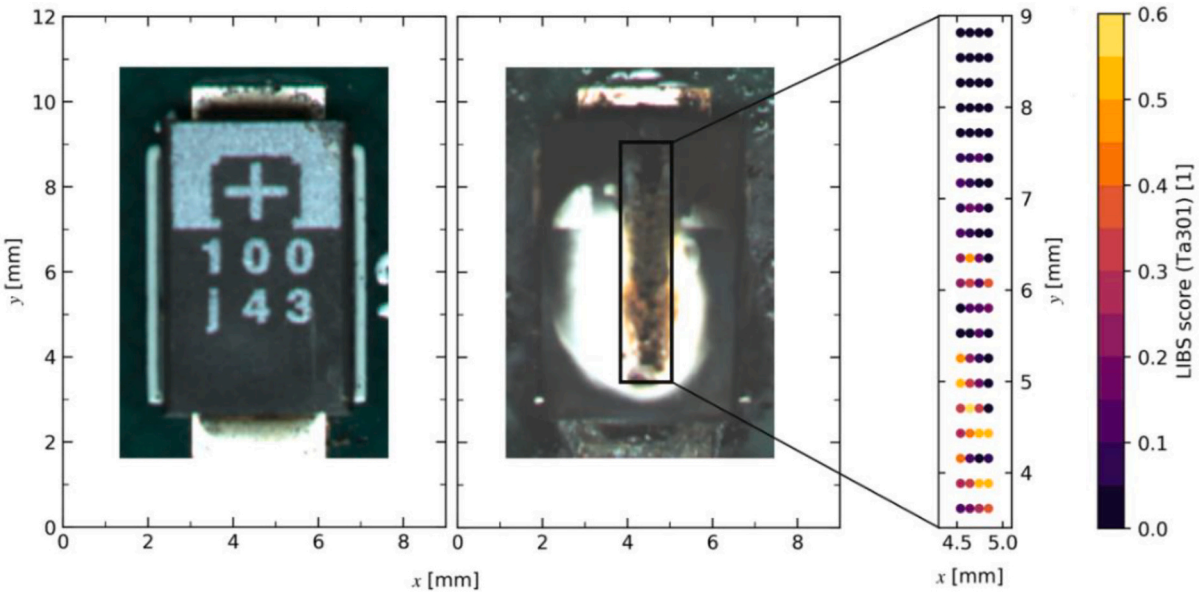

Fig. 6. Left: Picture of a SMD tantalum capacitor. The plus sign shows the position of the anode. Center: Picture of the same component after local penetration of the housing with laser ablation pulses, the result is a trench parallel to the longitudinal axis of the component (*y*-axis). Right: LIBS scores for tantalum in a raster scan of 20 × 4 measurement points within the trench. The rightmost color scale shows the respective values of the LIBS score in the range from 0 to 0.6.

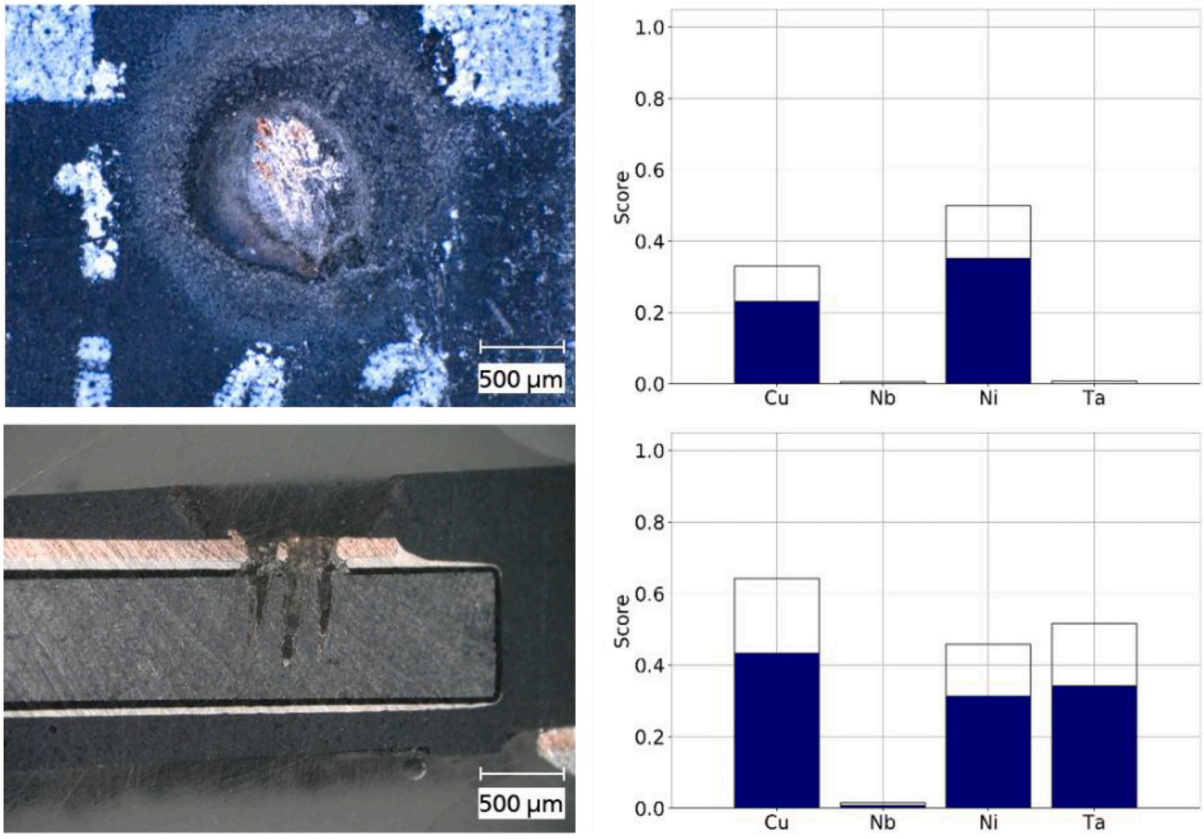

Fig. 7. Measurement results for a tantalum capacitor with LIBS measuring pulses (top row) and a sequence of ablation pulses followed by LIBS measuring pules (bottom row). Top left: view from above of crater when only 10 LIBS pulses were irradiated. Top right: LIBS scores for target analytes Cu, Nb, Ni and Ta for LIBS pulses only. Bottom left: cross section image of crater after irradiation of ablation pulses in a 3 × 3 raster (0.5 s ablation time per spot) and 10 LIBS pulses to the raster center. Bottom right: determined LIBS scores after pre-ablation (open bars: mean value; filled bars: mean minus std. dev.)

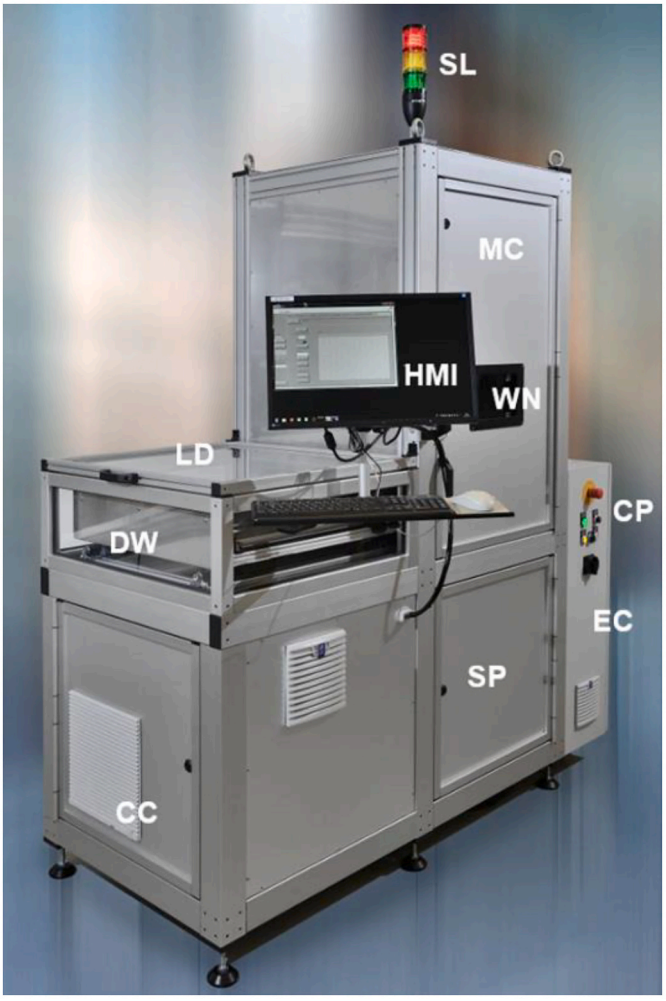

Fig. 8. Scanning LIBS set-up with 2D, 3D geometry measurements. EC electric cabinet with supply for scanner, axes and control electronics; CP control panel; CC control computer, laser cooler, laser power supply; SP multi-CCD spectrometer; LD lid to be opened to load the drawer (translation stage); DW drawer to charge the measuring objects; MC measuring cabinet with 2D, 3D cameras, scanner, laser source; SL signal light; HMI touch screen; WN observation window according to laser safety requirements.

electronic component (LIBS score surpasses a threshold, which refers to a score value being specific for the category of electronic component. This threshold is defined by the user for the particular application case), b) volume of the electronic component (deduced from the 2D-, 3D-measurements; yields an indirect measure of the total quantity of valuable material to be expected), c) data basis from representative conventional chemical analyses of valuable electronic components (provides e.g. the average content of tantalum oxide in dielectrics of tantalum capacitors), d) market price of valuable material for recycling. The following main target elements were considered: tantalum, neodymium, tungsten, gold, silver, platin group metals.

5. LIBS measuring system as part of an inverse production line

Fig. 8 shows the LIBS system in its configuration for the integration in an inverse production line [16]. All components of the set-up shown in Fig. 2 are built-in a closed housing to enable operation as laser class 1 system. The lid shown in Fig. 8 (LD) is used only for manual loading or taking out of measuring objects. For the LIBS system integrated in the inverse production line the loading and unloading is executed automatically by a manipulator system (LD is removed for this operation mode).

Fig. 9 shows a sketch of the whole inverse production line where the LIBS system is a part of (see no. 5, rightmost) as set-up in the ADIR project [1]. If cell phones are processed the sequence is as follows: 1) feeding and singularization, the pieces are transported on a belt conveyor to the next station; 2) position and orientation of incoming piece is recognized by a camera and a robot picks and transfers the cell phone in a processing station where the housing is opened, the battery is taken out and allocated to a first sorting fraction and finally the PCB is extracted and placed in a take-over station; 3) a manipulator picks this item and transfers it to the LIBS system if no sufficient data are available to decide which components shall be dismantled; if data can be recalled from a data base, the manipulator transfers the item directly to the desoldering station; 4) in the desoldering station the PCB is clamped on a *xy*-stage and a processing laser beam is scanned across the soldering pads of a component to be extracted, then the component is sucked off and transported to the corresponding sorting fraction (as e.g. a fraction for tantalum capacitors); for this action, data gained in a training phase by the system shown in Fig. 8 and fed to the data base are used; the laser can as well be operated in such a way to cut out integrated circuits (IC) from the board and to feed a further sorting fraction for these components; 5) 2D, 3D-geometry measurement of the PCB and LIBS measurements as described above, see Figs. 2, 3 and 7; 6) residual PCBs are further fragmented in a pulsed-power machine; 7) output fragments undergo an optical recognition to identify and take out vibration alerts (to recover tungsten)

Table 7 shows results of field test campaigns with respect to the sorting fractions of tantalum capacitors, surface acoustic wave filters and integrated circuits (ICs).

Tests have been executed to recover the valuable materials from the highly enriched sorting fractions gained with the inverse production line [17]. Recovery rates of the applied hydrometallurgical and pyrometallurgical processes were determined by putting the weight of the refined output material in relation to the weight and composition of the input material, i.e. the sorting fractions. In the case of Ta 97.7% were recovered from the fraction of capacitors. The other recovery rates are as follows: gold 98%, silver >96%, neodymium 96%, tungsten 96%.

6. Conclusions

For the first time a scanning LIBS method was developed to map the location of valuable elements inside electronic components on PCBs. High-resolution 2D- and 3D-data of the measuring object are obtained in the same set-up and deployed to control the deflection and focusing of the LIBS laser beam. The scan field for LIBS measurements by beam deflection amounts up to 500 × 500 mm^2, which is by orders of magnitude larger than those achieved so far. Selected electronic components can be targeted and measured by a sequence of ablation and analyzing laser pulses. Thus, the valuable interior parts of electronic components are accessed and LIBS score values of target elements are determined.

Based on this method a LIBS system was set-up and integrated in the worldwide first inverse production line. Field tests showed that the volume and composition of valuable electronic components on PCBs can be measured inline in automated process sequences.

The presented methodology proves, that LIBS is a suitable analysis tool for the realization of inverse production lines and thus a key enabling technology to close raw material flows and ultimately to achieve a sustainable circular economy.

Declaration of Competing Interest

None.

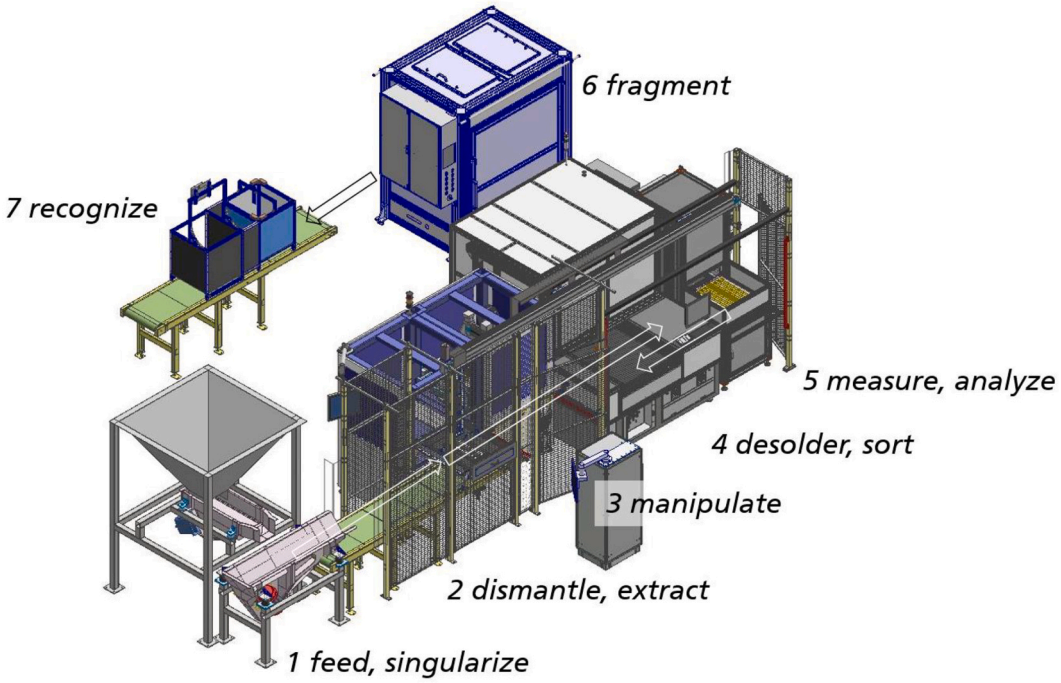

Fig. 9. Inverse production line as set-up in the ADIR project comprising seven machines to implement the handling, manipulation, measuring and processing of cell phones and PCBs from computers and servers, see text.

Table 7
Masses of sorting fractions generated by the inverse production line shown in Fig. 9.

Input material	No. of items	Masses of sorting fractions [g]
Cell phones	1080	Ta-capacitors 6675
Server PCBs	816	surface acoustic wave filters 54
		ICs 1286

Acknowledgement

The authors express their thanks for the support and funding of the ADIR project by the EU. This project has received funding from the European Union's Horizon 2020 research and innovation programme under grant agreement No. 680449.

The authors want to express their special thanks for all team members of the ADIR project who contributed with their R&D, laboratory, workshop and management work to the progress of the project including among many others: P. Balhorn, K. Bergmann, S. Connemann, R. Fleige, J. Vieker, Fraunhofer ILT, Aachen, Germany; T. Felsch, G. Strauss, A. Pomraenke, E. Schulenburg, S. Bexten, C. Walter, T. Kelm, Fraunhofer IFF, Magdeburg, Germany; C. Gehlen, V. Mörkens, J. Makowe, Laser Analytical Systems & Automation GmbH, Aachen, Germany; A. Tori, M. Guolo, OSAI A.S. S.p.A., Parella, Italy; N. Giorgetti, J. Merirand, Tau Industrial Robotics, Torino, Italy; A. Chmielarz, G. Benke, T. Gorewoda, K. Leszczyńska-Sejda, W. Kurylak, Lukasiewicz Research Network - Instytut Metali Niezelaznych, Gliwice, Poland; M. Bergamos, G. Sellin, Electrocycling GmbH, Goslar, Germany; H. Brumm, H.C. Starck Tantalum and Niobium GmbH, Goslar, Germany; M. Eschen, Aurubis AG, Lünen, Germany.

References

[1] EU project "Next generation urban mining – automated disassembly, separation and recovery of valuable materials from electronic equipment", 2018-2020, Grant Agreement no. 680449, www.ADIR.eu, 2021.

[2] M. Stepputat, R. Noll, On-line detection of heavy metals and brominated flame retardants in technical polymers with laser-induced breakdown spectrometry, Appl. Opt. 42 (2003) 6210–6220.

[3] M. Aguirre, M. Hidalgo, A. Canals, J. Nobrega, E. Pereira-Filho, Analysis of waste electrical and electronic equipment (WEEE) using laser-induced breakdown spectroscopy (LIBS) and multivariate analysis, Talanta 117 (2013) 419–424.

[4] F. Aquino, E. Pereira-Filho, Analysis of the polymeric fractions of scrap from mobile phones using laser-induced breakdown spectroscopy: Chemometric applications for better data interpretation, Talanta 134 (2015) 65–73.

[5] V. Costa, F. Aquino, C. Paranhos, E. Pereira-Filho, Identification and classification of polymer e-waste using laser-induced breakdown spectroscopy (LISS) and chemometric tools, Polym. Test. 59 (2017) 390–395.

[6] V. Costa, F. Aquino, C. Paranhos, E. Pereira-Filho, Use of laser-induced breakdown spectroscopy for the determination of polycarbonate (PC) and acrylonitrile-butadiene-styrene (ABS) concentrations in PC/ABS plastics from e-waste, Waste Manag. 70 (2017) 212–221.

[7] V. Costa, J. Castro, D. Andrade, D. Babos, J. Garcia, M. Speranca, T. Catelani, E. Pereira, Laser-induced breakdown spectroscopy (LIBS) applications in the chemical analysis of waste electrical and electronic equipment (WEEE), Trends Anal. Chem. 108 (2018) 65–73.

[8] J. Castro, E. Pereira, R. Bro, Laser-induced breakdown spectroscopy (LIBS) spectra interpretation and characterization using parallel factor analysis (PARAFAC): a new procedure for data and spectral interference processing fostering the waste electrical and electronic equipment (WEEE) recycling process, J. Anal. Atomic Spectr. 35 (2020) 1115–1124.

[9] D. Babos, A. Cruz-Conesa, E. Pereira Filho, J. Anzano, Direct determination of Al and Pb in waste printed circuit boards (PCB) by laser-induced breakdown spectroscopy (LIBS): evaluation of calibration strategies and economic-environmental questions, J. Hazard. Mater. 399 (2020) 122831.

[10] T. Kim, C. Lin, Y. Yoon, Compositional mapping by laser-induced breakdown spectroscopy, J. Phys. Chem. B 102 (1998) 4284–4287.

[11] L. Cabalin, M. Mateo, J. Laserna, Chemical maps of patterned samples by microline-imaging laser-induced plasma spectrometry, Surf. Interface Anal. 35 (2003) 263–267.

[12] F. Aquino, J. Santos, R. Carvalho, J. Coelho, E. Pereira-Filho, Obtaining information about valuable metals in computer and mobile phone scraps using laser-induced breaddown spectroscopy (LIBS), RSC Adv. 5 (2015) 67001–67010.

[13] R. Carvalho, J. Coelho, J. Santos, F. Aquino, R. Carneiro, E. Pereira-Filho, Laser-induced breakdown spectroscopy (LIBS) combined with hyperspectral imaging for the evaluation of printed circuit board composition, Talanta 134 (2015) 278–283.

[14] M. Speranca, A. Virgilio, E. Pereira-Filho, F. Aquino, Determination of elemental content in solder mask samples used in printed circuit boards using different spectroanalytical techniques, Appl. Spectrosc. 72 (2018) 1205–1214.

[15] R. Noll, G. Benke, M. Bergamos, H. Brumm, M. Eschen, C. Fricke-Begemann, K. Leszczynska-Sejda, J. Makowe, F. Schreckenberg, A. Tori, F. Veglia, Interlinked machinery for the automated disassembly, separation and recovery of valuable materials from electronic equipment – progress of the ADIR project, in: European

Metallurgical Conf., EMC 2019 3, 2019, pp. 1209–1225, sustainable production, ISBN 978–3–940276-89-6.

[16] Verfahren und Vorrichtung zur automatisierten Identifikation, Demontage, Vereinzelung und Sortierung von Komponenten elektronischer Baugruppen und Geräte für das werkstoffliche Recycling mit Laserstrahlung, grant of patent 15.10.2015.

[17] R. Noll, K. Bergmann, C. Fricke-Begemann, F. Schreckenberg, Inverse Produktion für nachhaltige Wertstoffkreisläufe – Aktuelle Entwicklungen zur automatisierten Demontage und Entstückung von Elektronikplatinen, Chem. Ing. Techn. 92 (2020) 360–367.

[18] A. Kramida, Y. Ralchenko, J. Reader, NIST ASD Team, *NIST Atomic Spectra Database* (ver. 5.8). https://physics.nist.gov/asd, 2021, April 26, National Institute of Standards and Technology, Gaithersburg, MD, , https://doi.org/10.18434/T4W30F.